Strangeness production in Au+Au collisions at $\sqrt{s_{NN}}$ = 14.6, 19.6, and 200 GeV with the STAR experiment

Yi Fang[1,*] (for the STAR collaboration)

[1]Tsinghua University, Beijing 100084 China

Abstract. Strangeness production has been suggested as a sensitive probe to the early dynamics of the deconfined matter created in heavy-ion collisions. In this presentation, we report new measurements of strange hadron (K^0_s, Λ, $\bar{\Lambda}$, Ξ, $\bar{\Xi}$, ϕ) production in Au+Au collisions at $\sqrt{s_{NN}}$ = 14.6, 19.6 GeV from STAR BES-II and $\Omega(\bar{\Omega})$ production in Au+Au collisions at $\sqrt{s_{NN}}$ = 200 GeV, including rapidity spectra, nuclear modification factors $R_{\rm CP}$ and Ω-to-ϕ ratios. Benefiting from the iTPC upgrade, the strangeness measurements are now extended from mid-rapidity (|y| < 0.5, BES-I) to a larger rapidity range (|y| < 1.0).

1 Introduction

The heavy-ion collisions at top Relativistic Heavy Ion Collider (RHIC) energy aim to study properties of QGP. The main motivations of the Beam Energy Scan (BES) program at RHIC are to search for the onset of deconfinement, search for the first-order phase transition and search for the critical point [1–3].

Strangeness production has been suggested as a sensitive probe to the early dynamics of the deconfined matter created in heavy-ion collisions. Ratios of particle yields involving strange particles are often utilized to study various properties of the nuclear matter, such as the strangeness and baryon chemical potentials (μ_S and μ_B) at the chemical freeze-out temperature ($T_{\rm ch}$). In addition, strange baryon-to-meson ratios can be utilized to test hadronization model predictions and understand the hadronization mechanism. The rapidity spectra of (anti-) strange baryons with larger rapidity acceptance of STAR detector give insight on the baryon stopping mechanism.

Measurements from STAR BES-I have indicated potential changes in the medium properties with decreasing collision energy [4]. However, the precision of those measurements is not sufficient to draw definitive conclusions. During BES-II, STAR has accumulated high statistics data in Au+Au collisions at various energies, which have 10-20 times higher statistics than BES-I and could help reduce the uncertainties in the strange hadron measurements, in particular for the multi-strange hadrons. In this contribution, we present new STAR measurements of strange hadron (K^0_s, Λ, $\bar{\Lambda}$, Ξ, $\bar{\Xi}$, ϕ) production in Au+Au collisions at $\sqrt{s_{NN}}$ = 14.6, 19.6 GeV from BES-II and $\Omega(\bar{\Omega})$ production in Au+Au collisions at $\sqrt{s_{NN}}$ = 200 GeV, and compare the new results with BES-I and model predictions. New insights on the collision dynamics is discussed.

*e-mail: fy21@mails.tsinghua.edu.cn

2 Experiment and analysis details

The datasets of Au+Au collisions at $\sqrt{s_{NN}}$ = 14.6, 19.6 and 200 GeV were collected in 2019 with the STAR detector, which has large and uniform acceptance and excellent particle identification. The main sub-detectors used in this analysis are the Time Projection Chamber (TPC) and Barrel Time-of-Flight Detector (BTOF). The upgraded inner TPC (iTPC) enlarges η coverage from 1.0 to 1.5 and decreases the p_T threshold from 120 MeV to 60 MeV. The charged particle identification is accomplished by measuring the $\langle dE/dx \rangle$ with the TPC and using the BTOF information. The daughter particles $\pi^{\pm}$, $K^{\pm}$, and $p(\bar{p})$ are used to reconstruct the secondary vertex of strange particles $K^0_S, \Lambda(\bar{\Lambda}), \Xi^-(\bar{\Xi}^+), \Omega^-(\bar{\Omega}^+)$ except for ϕ which is assumed to originate from the primary vertex due to its very short lifetime. The large number of reconstructed strange particles allow multi-differential measurements.

3 Results and discussion

3.1 Rapidity spectra

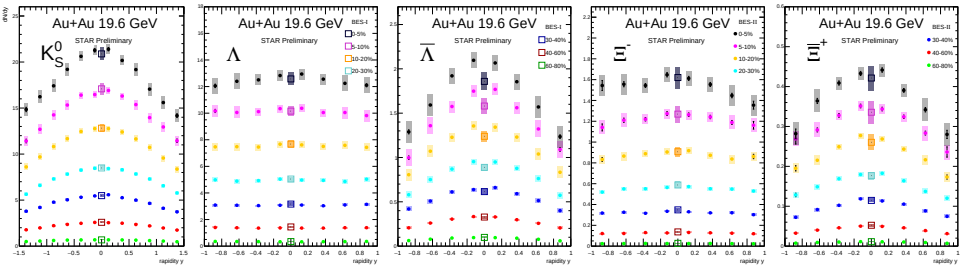

Figure 1: The rapidity spectra of $K^0_S, \Lambda(\bar{\Lambda})$ and $\Xi^-(\bar{\Xi}^+)$ in Au + Au collisions at $\sqrt{s_{NN}}$ = 19.6 GeV, for different centrality ranges. The systematic errors are shown as colored boxes, while the statistical errors are shown as vertical lines. The solid points are from BES-II data while the open points are published results from BES-I [4]

.

The transverse-momentum (p_T) spectra of strange hadrons are obtained by correcting the raw yields, extracted from the invariant mass distributions in a given invariant mass window, by the reconstruction efficiencies. The full p_T-integrated yields (dN/dy) versus rapidity of $\Lambda(\bar{\Lambda}), \Xi^-(\bar{\Xi}^+), \Omega^-(\bar{\Omega}^+), \phi$ are obtained by extrapolating the measured p_T spectra. The K^0_S can be measured down to p_T equal to 0, therefore the extrapolation is not necessary. Benefiting from the iTPC upgrade, the strangeness measurements are now extended from mid-rapidity ($|y| < 0.5$) to a larger rapidity range ($|y| < 1.0$). The rapidity of K^0_S can be measured up to 1.5 ($|y| < 1.5$). STAR have accumulated high statistics data which allows to extract the rapidity distribution within $\Delta y = 0.25$ intervals. Figure 1 shows the rapidity spectra of strange hadrons ($K^0_S, \Lambda, \bar{\Lambda}, \Xi^-, \bar{\Xi}^+$) at $\sqrt{s_{NN}}$ = 19.6 GeV which demonstrates the acceptance of iTPC. The open symbols represent data from BES-I [4], while the closed symbols represent the preliminary data from BES-II. The BES-II results are consistent with BES-I.

Figure 1 shows that the rapidity spectra of mesons (K^0_S) and anti-baryons ($\bar{\Lambda}, \bar{\Xi}^+$) are Gaussian-like distributions, while the rapidity distribution of baryons (Λ, Ξ^-) are broader than that of anti-baryons ($\bar{\Lambda}, \bar{\Xi}^+$) in Au+Au collisions, this is mainly due to the extra contributions from stopped baryons. At $\sqrt{s_{NN}}$ = 19.6 GeV, the incident nucleons at beam rapidity could

not be completely stopped at rapidity y=0, which gives rise to a distinct minimum of the rapidity distribution of net baryon at mid-rapidity [5]. Meanwhile, baryons and anti-baryons can be produced via pair production at this energy. Due to these two competing effects, the distributions for baryons show a plateau at mid-rapidity, while the distributions for anti-baryons are Gaussian-like. And the similar trends also have been observed by the NA49 collaboration [5].

3.2 Nuclear modification factor at $\sqrt{s_{NN}}$ = 19.6 and 14.6 GeV

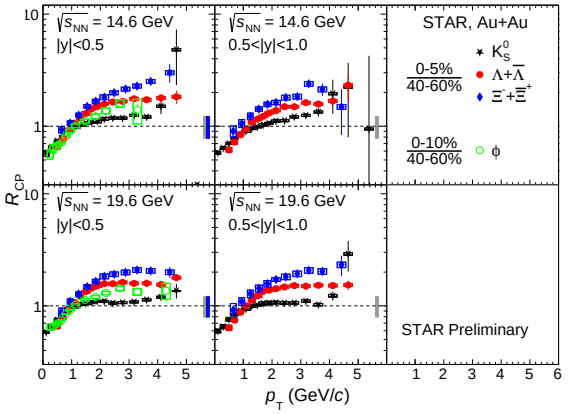

Figure 2: K^0_S, $\Lambda + \bar{\Lambda}$, $\Xi^- + \bar{\Xi}^+$ R_{CP} (0-5%)/(40-60%), and ϕ R_{CP} (0-10%)/(40-60%), at midrapidity (|y| < 0.5) and larger rapidity (0.5 < |y| < 1.0) in Au + Au collisions at $\sqrt{s_{NN}}$ = 14.6 and 19.6 GeV. The vertical bars represent the statistical errors and the box on those data points of K^0_S, Λ, Ξ represent the systematic errors. The blue and gray bands on the right side of those panels respectively represent the normalization uncertainties from $N_{\rm coll}$ for R_{CP} (0-10%)/(40-60%) and R_{CP} (0-5%)/(40-60%).

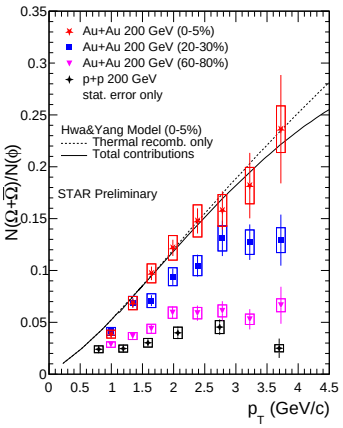

Figure 3: Baryon-to-meson ratio, $(N\left(\Omega^- + \bar{\Omega}^+\right)/[2N(\phi)])$, as a function of p_T at midrapidity (|y| < 0.5) in Au + Au collisions at $\sqrt{s_{NN}}$ = 200 GeV. The ϕ data are from the published STAR result [6]. The vertical bars represent the statistical errors and the box represent the systematic errors.

Figure 2 shows the nuclear modification factor, R_{CP} of $K^0_S, \Lambda(\bar{\Lambda}), \Xi^-(\bar{\Xi}^+)$ in Au+Au collisions at $\sqrt{s_{NN}}$ = 14.6, 19.6 GeV, the definition of R_{CP} is the ratio of particle yield in central collisions to that in peripheral collisions, which is scaled by the average number of inelastic binary collisions $\langle N_{\rm coll} \rangle$,

$$R_{\rm CP} = \frac{[(dN/dp_T) / \langle N_{\rm coll} \rangle]_{\rm central}}{[(dN/dp_T) / \langle N_{\rm coll} \rangle]_{\rm peripheral}} \quad (1)$$

R_{CP} is unity if nucleus-nucleus collisions are just simple superpositions of nucleon-nucleon collisions. Figure 2 shows that the R_{CP} tends to be flat and larger than unity at p_T > 2 GeV/c. This enhancement in this p_T region may be due to radial flow and/or the relative dominance of coalescence versus fragmentation for hadronization. The enhancement

is stronger for Ξ^- compare to Λ and K^0_S. It is worth noting that strong enhancement for multi-strange particles is a proposed signature for QGP formation. The R_{CP} at mid-rapidity($|y| < 0.5$) is similar at larger rapidity ($0.5 < |y| < 1.0$), indicating minor rapidity dependence.

3.3 Ω/ϕ ratio at $\sqrt{s_{NN}}$ = 200 GeV

Figure 3 shows the Ω/ϕ ratio measured in Au + Au collisions at $\sqrt{s_{NN}}$ = 200 GeV in the centrality of 0–5%, 20–30% and 60–80%. The dashed lines and the solid lines respectively represent recombination model calculations for central collisions with thermal and total strange quark contributions [7, 8]. The ratios are in good agreement with coalescence and recombination dynamics over the p_T range of 1-4 Gev/c in central collisions (0-5%), which suggests that Ω and ϕ are predominantly produced through the recombination of thermalized strange quark in QGP. From the small systems (peripheral collisions) to large systems (central collisions), the ratio increases gradually with increasing system size at intermediate p_T. Significant Ω enhancement over ϕ is observed in central collisions with respect to peripheral collisions. The black marker is the Ω/ϕ ratio in p+p collision at $\sqrt{s_{NN}}$ = 200 GeV, which is close to that in peripheral Au+Au collisions, hinting there may be smooth transition from p+p collisions to Au+Au collisions.

4 Summary

In these proceedings, we present the new STAR measurements of strangeness production with extended p_T and rapidity coverages. The analyzed datasets are taken from Au+Au collisions at BES-II energies ($\sqrt{s_{NN}}$ = 14.6 and 19.6 GeV) and $\sqrt{s_{NN}}$ = 200 GeV. The rapidity spectra of baryons(Λ, Ξ^-) are broader than those of the anti-baryons($\bar{\Lambda}, \bar{\Xi}^+$) at $\sqrt{s_{NN}}$ = 14.6 and 19.6 GeV, likely due to extra contributions from stopped baryons. The baryon enhancement is observed at $\sqrt{s_{NN}}$ = 14.6, 19.6 and 200 GeV, which is consistent with QGP formation at these energies. In addition, significant Ω enhancement over ϕ is observed in central Au+Au collision at $\sqrt{s_{NN}}$ = 200 GeV, indicating that Ω and ϕ are predominantly produced through the recombination of thermalized strange quark in QGP. The Ω/ϕ ratio decrease from central to peripheral Au+Au collisions, which is similar to that in p+p collisions, hinting there may be smooth transition from p+p collisions to Au+Au collisions.

References

[1] M. A. Stephanov, Prog. Theor. Phys. Suppl. **153**, 139-156 (2004)
[2] B. Mohanty, Nucl. Phys. A **830**, 899C-907C (2009)
[3] M. M. Aggarwal *et al.* [STAR], [arXiv:1007.2613 [nucl-ex]].
[4] J. Adam *et al.* [STAR], Phys. Rev. C **102**, no.3, 034909 (2020)
[5] C. Alt *et al.* [NA49], Phys. Rev. C **78**, 034918 (2008)
[6] B. I. Abelev *et al.* [STAR], Phys. Rev. Lett. **99**, 112301 (2007)
[7] R. C. Hwa and C. B. Yang, Phys. Rev. C **66**, 025205 (2002)
[8] R. C. Hwa and C. B. Yang, Phys. Rev. C **75**, 054904 (2007)